Simulation of the electromagnetic field in a cylindrical cavity of an ECR ions source

IOP Conf. Series: Journal of Physics: Conf. Series **935** (2017) 012073 doi:10.1088/1742-6596/935/1/012073

Simulation of the electromagnetic field in a cylindrical cavity of an ECR ions source

A Estupiñán[1], E A Orozco[1], V D Dugar-Zhabon[1] and M T Murillo Acevedo[3]

[1] Universidad Industrial de Santander, Bucaramanga, Colombia
[2] Universidad Manuela Beltrán, Bucaramanga, Colombia
[3] Universidad Santo Tomás, Bucaramanga, Colombia

E-mail: alex.estupinan@saber.uis.edu.co

Abstract. Now there are numerous sources for multicharged ions production, each being designed for certain science or technological objectives. Electron cyclotron resonance ion sources (ECRIS) are best suited for designing heavy ion accelerators of very high energies, because they can generate multicharged ion beams at relatively great intensities. In these sources, plasma heating and its confinement are effected predominantly in minimum-B magnetic traps, this type of magnetic trap consist of two current coils used for the longitudinal magnetic confinement and a hexapole system around the cavity to generate a transversal confinement of the plasma. In an ECRIS, the electron cyclotron frequency and the microwave frequency are maintained equal on a quasi-ellipsoidal surface localized in the trap volume. It is crucial to heat electrons to energies sufficient to ionize K- and L- levels of heavy atoms. In this work, we present the preliminary numerical results concerning the space distribution of TE_{111} microwave field in a cylindrical cavity. The 3D microwave field is calculated by solving the Maxwell equations through the Yee's method. The magnetic field of minimum-B configuration is determined using the Biot-Savart law. The parameters of the magnetic system are that which guarantee the ECR surface location in a zone of a reasonably high microwave tension. Additionally, the accuracy of electric and magnetic fields calculations are checked.

1. Introduction

Initially, the Electron Cyclotron Resonance Ions Sources (ECRIS) were elaborated and fabricated as a heavy particle injection part for cyclotron systems [1]. Harnessing of the low-emittance multicharged ion beams in cyclotron accelerators permits to achieve high energies that are quadratic in the ion charge. Thereafter the ECRIS found its application in the ion implantation technology, mass-spectrometry, technology of Nano layer production, low-impulse propulsion engines, etc. [2–5]. The conditions and processes that lead to multicharged ion generation in ECRIS is discussed in [1, 6–9]. Of all the parameters that determine the ion yield and the ion charge states, two of them are of importance: the magnetostatic field profile and microwave field distribution in the trap volume, especially the ECR zone location in the magnetostatic trap field. In this work, we present some results on the numerical simulation of the TE_{111} microwave field in a cylindrical resonant cavity of 10 *cm* long and 9.1 *cm* in diameter, which is typical of some real ECRIS. Calculating the magnetic field it is important to keep in mind that the ECR zone should be as large as possible but should not touch the cavity walls. This trap field is determined using the Biot-Savart law [10].

2. Theoretical formalism

A physical scheme of a typical ECRIS is shown in Figure 1(a).The ECR plasma is confined by the minimum-B magnetic field formed by two current coils (1) and the hexapole permanent magnet system (2). The discharge chamber (3) made of copper is placed inside the magnetic system. The discharge chamber is fed by microwaves from a magnetron generator along the chamber axis (4),(5) y (6). In our case, a microwave fed line transversal to the chamber axis is used, being presented in Figure 1(b). In this scheme, two current coils (7) are disposed bilaterally symmetrical with the cavity (1). The hexapole bars (6) are set on the cavity cylinder surface parallel to each other in such a way that the fed line passes between the bars. The magnetic system is shown in Figure 1(b).

The fed line consists of a 2.45 GHz magnetron mounted on a waveguide that relates to the chamber through a rectangular window of $7.65 \times 1.0\ cm^2$ in size.

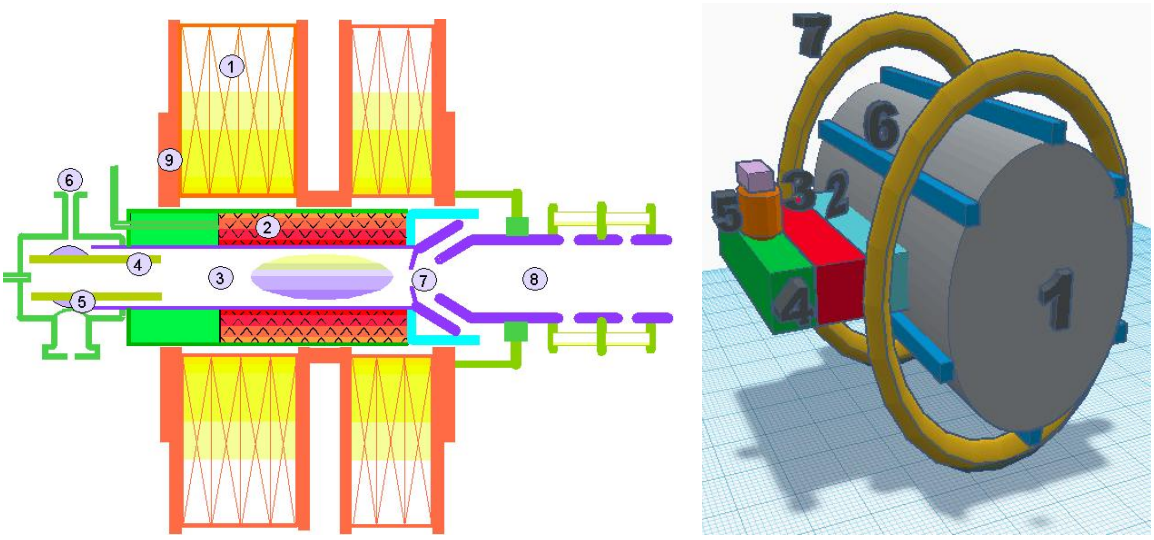

(a) (b)

Figure 1. (a) Schematic diagram of the ECR ion source: 1-coils, 2-hexapole, 3-plasma chamber, 4-coaxial line, 5-tuner, 6-RF injection, 7-exit hole, 8-Einzel lens, 9-yoke. (Figure taken from [11]). (b) Three-dimensional physical scheme of the simulate system: 1-cavity, 2-window, 3-ferrite isolator, 4-waveguide, 5-magnetron, 6-hexapole, 7-coils.

The electromagnetic field evolution in the cavity is calculated by using the UPML method, where the fields components evolve according to the next set of equations [12]:

$$\frac{\partial H_z}{\partial y} - \frac{\partial H_y}{\partial z} = \frac{\partial}{\partial t}(K_y D_x) + \frac{\sigma_y}{\epsilon_0} D_x \tag{1}$$

$$\frac{\partial H_x}{\partial z} - \frac{\partial H_z}{\partial x} = \frac{\partial}{\partial t}(K_z D_y) + \frac{\sigma_z}{\epsilon_0} D_y \tag{2}$$

$$\frac{\partial H_y}{\partial x} - \frac{\partial H_x}{\partial y} = \frac{\partial}{\partial t}(K_x D_z) + \frac{\sigma_x}{\epsilon_0} D_z \tag{3}$$

and

$$\frac{\partial E_z}{\partial y} - \frac{\partial E_y}{\partial z} = -\frac{\partial}{\partial t}(K_y B_x) - \frac{\sigma_y}{\epsilon_0} B_x \tag{4}$$

$$\frac{\partial E_x}{\partial z} - \frac{\partial E_z}{\partial x} = -\frac{\partial}{\partial t}(K_z B_y) - \frac{\sigma_z}{\epsilon_0} B_y \tag{5}$$

$$\frac{\partial E_y}{\partial x} - \frac{\partial E_x}{\partial y} = -\frac{\partial}{\partial t}(K_x B_z) - \frac{\sigma_x}{\epsilon_0} B_z \tag{6}$$

where:

$$\check{D}_x = \epsilon_0 \frac{S_z}{S_x} \check{E}_x \ , \ \check{D}_y = \epsilon_0 \frac{S_x}{S_y} \check{E}_y \ , \ \check{D}_z = \epsilon_0 \frac{S_y}{S_z} \check{E}_z \tag{7}$$

and

$$\check{B}_x = \mu \frac{S_z}{S_x} \check{H}_x \ , \ \check{B}_y = \mu \frac{S_x}{S_y} \check{H}_y \ , \ \check{B}_z = \mu \frac{S_y}{S_z} \check{H}_z \tag{8}$$

where

$$S_x = K_x + \frac{\sigma_x}{j\omega\epsilon_0} \ \ ; \ \ S_y = K_y + \frac{\sigma_y}{j\omega\epsilon_0} \ \ ; \ \ S_z = K_z + \frac{\sigma_z}{j\omega\epsilon_0}. \tag{9}$$

In our simulations K_x, K_y y K_z are chosen equal to the unity and the electrical conductivities $\sigma_x, \sigma_y, \sigma_z$ are chosen equal to zero in all space except the microwave port where $\sigma_x = (x/d)^3 \sigma_x^{max}$, $d = 10\Delta x$ is the width of the UPML with with the spatial step Δx in x direction, x is the distance from the border towards the interior of the UPML and $\sigma_x^{max} = 0.8(m+1)/(\Delta x\sqrt{\mu_0/\varepsilon_0})$ with $m = 3$ when 10 cells are used in the UPML zone as in this case. The UPML zone is used to avoid non physical reflections.

This set of equations (1)-(6) is written in a finite difference scheme using the Yee method and solved in the traditional way [13].

The static magnetic field of this trap is obtained by the superposition of the field produced by two systems. The first one is the coil magnetic field, where each coil is simulated as a superposition of circular turns with stationary current. The second one is the hexapole magnetic field. This field is calculated using the magnetic potential method because all hexapole magnets are out of the confinement region. The field produced for one turn in the point (x, y, z) in Gaussian units is:

$$\vec{B}(x,y,z) = \frac{RI}{c} \int_0^{2\pi} \frac{(cos\theta(z-z_s)\hat{i} + sin\theta(z-z_s)\hat{j} - [ysin\theta + xcos\theta - R]\hat{k})}{[(x^2+y^2-2R(xcos\theta + ysin\theta) + R^2 + (z-z_s)^2]^{3/2}} d\theta. \tag{10}$$

Where R is radius of turn, which center is along z axis at point $(0, 0, z_s)$, I is electric current and c is the light velocity [10].

The second one is the magnetic field from magnets which conform the sixtupole system. This magnetic field can be calculated through the method of gradient of scalar magnetic potential since, none magnet exists in confinement region [14]:

$$\phi_m(\vec{r}) = \int_{s_{(v)}} \frac{\vec{M}(\vec{r}')}{|\vec{r} - \vec{r}'|} \cdot d\vec{s}' - \int_v \frac{\nabla' \cdot \vec{M}(\vec{r}')}{|\vec{r} - \vec{r}'|} dv' \tag{11}$$

where ϕ_m is the scalar magnetic potential, $s_{(v)}$ is the magnet boundary surface, v is the magnet volume.

3. Results and discussion

The numerical simulation of the cavity microwave field is realized under the above-mentioned physical parameters. To excite a microwave field of 14 kV/cm tension, an input power of 569 kW is injected into the cavity through a TE_{10} waveguide. Such a high level of the microwave power are related with the use of an not optimal injection system for our simulations. For this system the quality factor of the cavity is too low (about 50). However, for an standard experimental system this quality factor may be of the order of 10000, therefore the same electric field strength inside the cavity could be obtained with a injection power of the order of kW. In the simulations, a perfect electric conductor (PEC) approximation is taken for describing the electrical characteristics of both the waveguide and cavity walls. Uniaxial perfectly matched layer (UPML) method [12] is applied for calculating the microwave power injected through the cavity window. The simulations are fulfilled on a rectangular 3D mesh at the spatial steps $\Delta x = \Delta y = 0.07\ cm, \Delta z = 0.2\ cm$ at a time step $\Delta t = 2.07\ ps$, that are chosen in accordance with the Courant stability condition [15].

In Figure 2(a) one can see the distribution of the electric field strength in the cavity middle cross section ($z = L_c/2$, L_c is the cavity length), and its vector pattern Figure 3 shows the electric field strength in longitudinal plane $y = 0$. There is an obviously good agreement between this distribution and the TE_{111} pattern that can be obtained from the well-known analytical expressions. The calculation accuracy of the electric and magnetic fields in the cavity obtained by solutions of $\nabla \cdot \vec{B} = 0$ and $\nabla \cdot \vec{E} = 0$, equations in a finite difference form is found no worse than to 10^{-7}.

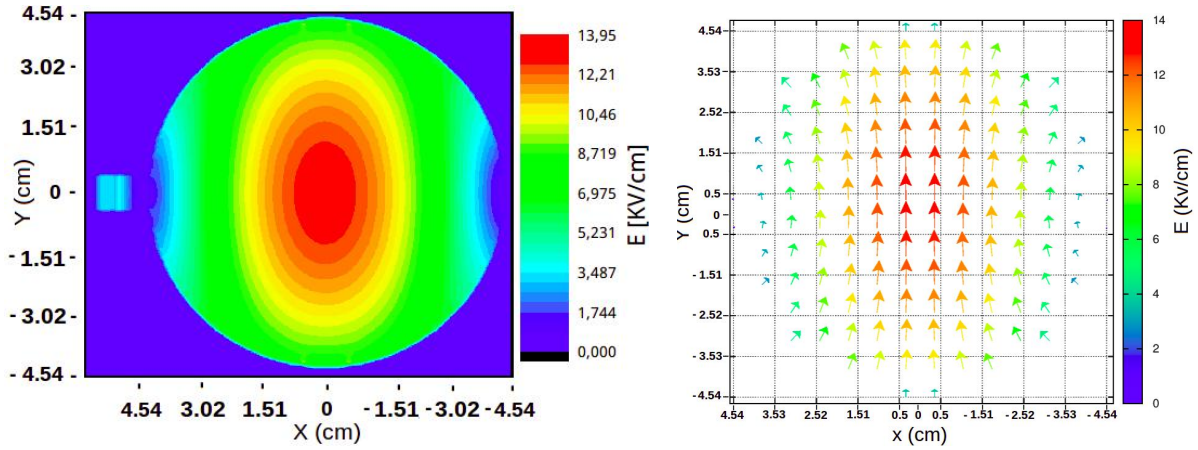

(a) (b)

Figure 2. (a) The electric field strength in the cross section $z = L_c/2$. (b) The corresponding electric vector field.

From electric field distribution presented in Figure 2 and Figure 3, it follows that the yellow zone corresponding to the electric field of order of 10 kV/cm is appropriate for resonance energizing of electrons. From this standpoint, it could be profitable if the ECR zone coincided with the yellow microwave zone. Two current coils and six permanent magnetic bars form the magnetic field of minimum-B type. The geometry of the coils and bars, the degree of bar magnetization and coil current are chosen so that the ECR zone $B(x, y, z) = (m\omega)/(-e) = 87.53\ mT$, coincides accurately with the yellow microwave zone (see Figure 2(a)). Here m and $-e$ are the electron mass and the magnitude of electric charge of electron, ω is the microwave angular frequency. The space shape of the ECR zone calculated in accordance with the above-mentioned method is shown in Figures 4. One can see from Figures 2 and Figures 4 that the

ECR and the microwave yellow zones do not coincide perfectly but the fact that the ECR zone oscillates around the yellow zone provides some expectations that no-coincidence of these zones has not an adverse effect on the ECR heating efficiency.

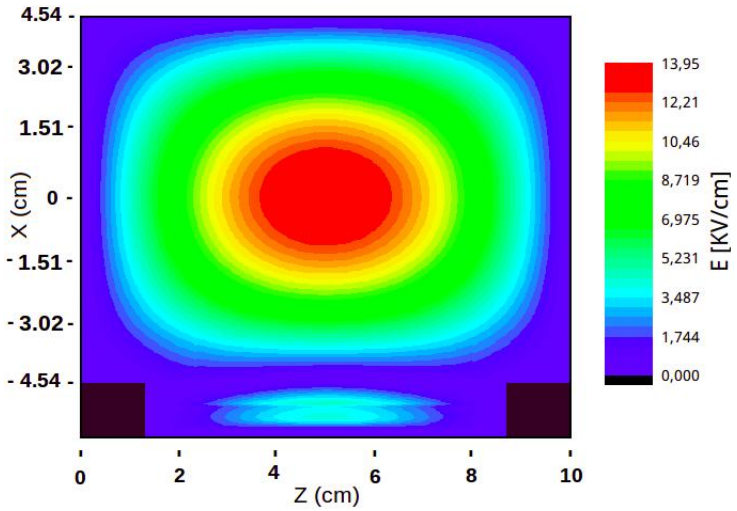

Figure 3. Electric field strength in the longitudinal plane $y = 0$.

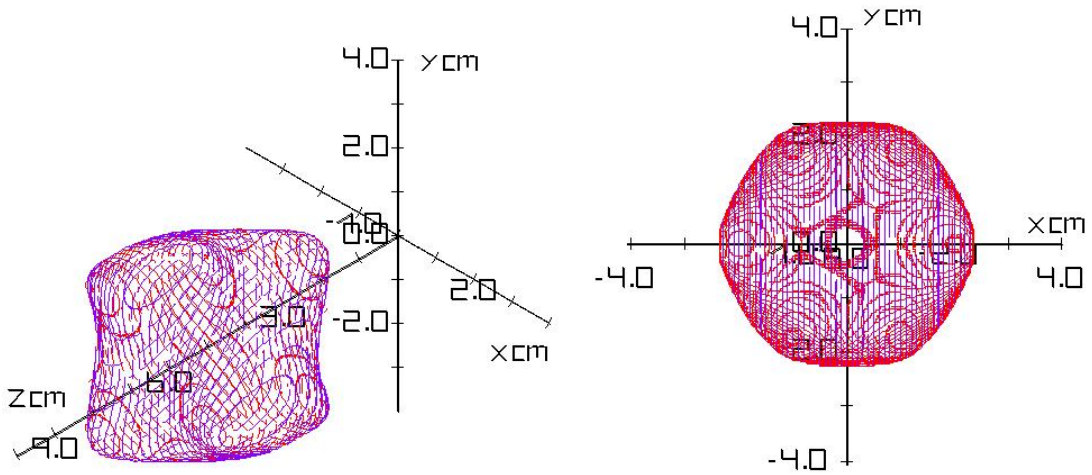

(a) (b)

Figure 4. (a) 3D view of the ECR Zone. (b) The ECR zone in the cross section $z = L_c/2$.

4. Conclusions

By choosing the trap magnetic field shape of ECR ion source, we proceed from the microwave field distribution in the TE_{111} cavity because it is much easier to manipulate the magnetic field shape than the microwave distribution in a cavity. It is shown that in the chosen minimum-B trap the ECR zone must be of an ellipsoidal type shape. In the near future, the numerical simulation of plasma heating in a minimum-B trap by the particle-in-cell method will be realized.

Acknowledgments
This work is supported by "Facultad de Ciencias and Escuela de Física, Universidad Industrial de Santander (UIS), Colombia".

References

[1] Geller R 1996 *Electron cyclotron resonance ion sources and ECR plasmas* (Bristol: Institute of Physics Publishing)
[2] Chen F F 2012 *Introduction to plasma physics* (New York: Springer International Publishing AG)
[3] Brown I G 2004 *The physics and technology of ion sources* (Germany: John Wiley & Sons)
[4] Kawai Y, Ikegami H, Sato N, Matsuda A and Uchino K 2010 *Industrial plasma technology: Applications from environmental to energy technologies* (Germany: John Wiley & Sons)
[5] Nakamura T and Riedmüller W 1974 *AIAA Journal* **12** 661–668
[6] Xie Z Q 1998 *Review of Scientific Instruments* **69** 625–630
[7] Dougar-Jabon V D, Umnov A M and Suescun Diaz D 2002 *Review of Scientific Instruments* **73** 629–631
[8] Dougar Jabon V D, Vivas F, Chacon Velasco A J and Umnov A M 1998 *Review of Scientific Instruments* **69** 671–673
[9] Dougar-Jabon V D, Umnov A M and B K V 1996 *Review of Scientific Instruments* **67** 1152–1154
[10] Murillo M T and Otero O 2016 vol 687 p 012022
[11] Burau H, Widera R, Honig W, Juckeland G, Debus A, Kluge T, Schramm U, Cowan T E, Sauerbrey R and Bussmann M 2010 *IEEE Transactions on Plasma Science* **38(10)** 2831–2839
[12] Taflove A and Hagness S C 2005 *Computational electrodynamics: The finite-difference time-domain method* (USA: Artech house Inc.)
[13] Yee K 1966 *IEEE Transactions on antennas and propagation* **14** 302–307
[14] Acevedo Murillo M T, Dugar-Zhabon V D and Otero O 2016 *Journal of Physics: Conference Series* vol 687 (IOP Publishing) p 012023
[15] Dugar-Zhabon V D, González J D and A O E 2016 vol 687 p 012077